AKADÉMIAI KIADÓ

Dual-energy CT in the emergency department: A pictorial essay from a single center experience

VINCENZO CIRIMELE*, GIULIA D'AMONE, CARLO MALLIO, BRUNO BEOMONTE ZOBEL and ELIODORO FAIELLA

Fondazione Policlinico Universitario Campus Bio-Medico, Rome, Italy

Received: May 21, 2023 • Revised manuscript received: October 24, 2023 • Accepted: November 26, 2023

IMAGING

PICTORIAL ESSAY

ABSTRACT

Learning Objectives: To provide a pictorial review of the main clinical applications of DECT with a focus on traumatic and non-traumatic emergencies.

Methods: DECT is becoming increasingly common in clinical practice. The differences in attenuation between two different datasets allow to perform a qualitative and quantitative characterization of the materials contained in a single voxel. Virtual monoenergetic images, material decomposition images, electron density maps, and atomic number maps are created by post-processing algorithms and offer the radiologist useful diagnostic data.

Results: We present a series of cases illustrating the utility of DECT in the diagnosis and management of acute pathologies, with a special focus on musculoskeletal imaging and neuroimaging.

Conclusion: DECT is a useful imaging technique that may allow radiologists to make quicker and more precise diagnoses in the emergency setting.

KEYWORDS

dual-energy CT, tomography spiral computed, emergency department, iodine map, metal artifact, uric acid

Learning objective

The presentation's objective is to present a pictorial review of the main clinical applications of DECT in both traumatic and non-traumatic emergencies, in order to illustrate its added value in the emergency department and its usefulness for a better assessment of organ perfusion, tissue/lesion characterization, mass detection, and iodine quantification. In addition to supporting quick treatment decisions in many acute conditions without subjecting the patient to an increased radiation dose, spectral CT has improved diagnostic capabilities [1].

Methods

DECT is becoming increasingly common in clinical practice. It is based on the collection of two attenuation datasets with various x-ray photon energies. The photoelectric effect, which dominates at lower energy levels, and Compton scattering, which takes place at energies above 50 kiloelectron volts (keV), are the main sources of the attenuation coefficients.

There are several ways to obtain the two energy levels' datasets. The three main acquisition methods currently in use are dual source acquisition, rapid kV switching, and detector-based spectral separation. In the former, the detector is a dual-layer detector that separates the energy levels after the beam has crossed the patient, detecting low-energy photons in the top layer and high-energy photons in the bottom layer [2, 3].

Since the attenuation of a material depends on the atomic number, the electron density, and the energy of the X-ray beam, the differences in attenuation at two different datasets

IMAGING 15 (2023) 2, 94–100
DOI: 10.1556/1647.2023.00152

*Corresponding author.
Tel.: +39 3343309772.
E-mail: v.cirimele@policlinicocampus.it

enable qualitative and quantitative characterization of the materials contained in a single voxel. Post-processing algorithms create virtual monoenergetic images, material decomposition images, electron density maps, and effective atomic number maps, thus providing the radiologist with helpful diagnostic information [2, 4–7].

The main spectral acquisition techniques provide scans with comparable radiation doses to single-energy CT, regardless of the technique [8–10].

Our DECT exams were obtained using a Dual-Source multidetector CT scanner (Somatom Force; Siemens Healthcare, Forchheim, Germany). Unenhanced images were obtained using the following imaging protocol: 100/140 kV, mAs modulated with the CARE Dose4D plugin, slice thickness 0.6 mm, collimation 128 × 0.6 mm, pitch 0.7. Suggested kernels include sharp and soft reconstruction kernels (Br 44 and Br 69, respectively). DECT pulmonary angiography was performed after intravenous injection of 70 mL of contrast agent (Omnipaque 350 mg mL^{-1}; GE Healthcare).

DECT data were post-processed with Syngo.via workplace post-processing software. In our Institution, radiographers working in the Emergency Department are trained to use Syngo.via workstation, in order to do post-processing work in a short period of time while the radiologist is reporting the conventional exams. DECT images are then archived in our Picture Archiving and Communication System (PACS).

In BME images, for example, we obtain axial, sagittal and coronal reconstructions, where the zones of bone marrow edema are depicted in green. A 3D BME image is also generated. The entire post-processing workflow usually requires less than a minute. The same post-processing time is usually required for lung perfusion maps and urinary stone characterization. A useful tip would be to obtain DECT post-processed images in at least 2 planes, in order to avoid misinterpretation due to partial volume artifacts, especially in BME and iodine perfusion maps.

In our institution, we perform DECT of the musculoskeletal system every time there is a diagnostic doubt on conventional radiography. DECT pulmonary angiography is not routinely performed; we perform it when there is a specific request regarding the quantification of perfused lung parenchyma.

Regarding DECT radiation exposure, the use of advanced post-processing and iterative reconstruction algorithms allowed a radiation dose comparable to single-energy CT.

The image quality of DECT images is inferior to single-energy CT images because DECT images are generated from 50% of the total dose compared to SECT (single-energy CT). X-ray beams in DECT are polychromatic and cause higher image noise.

Results

The DECT scans were performed with a dual-source scanner (Siemens Somatom Force) equipped with two x-ray tubes working at two different energy levels (80 and 140 kVp).

We present a series of cases illustrating the utility of DECT in the diagnosis and management of acute pathologies. We describe the importance of DECT applications such as pointing out bone marrow edema, metal artifact reduction, urinary stone characterization, and iodine perfusion maps, highlighting their impact on patients' clinical management.

Case 1: multiple recent vertebral fractures showing bone marrow edema at DECT (Fig. 1). The patient was a 88-year-old man with multiple vertebral fractures detected at radiography. Fractures were confirmed by CT. DECT bone marrow images showed bone edema in T9, T10, T11 and T12 vertebral bodies, indicating recent osteoporotic fractures.

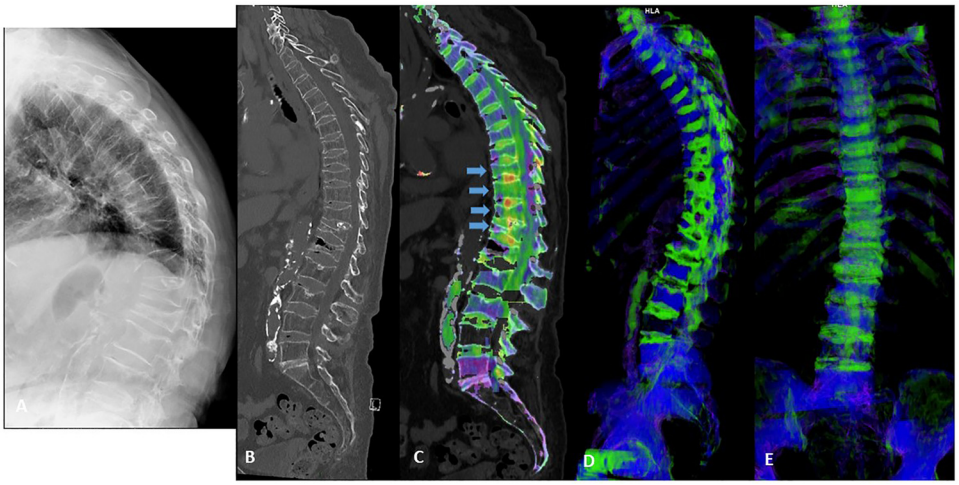

Fig. 1. 88-year-old patient with multiple vertebral fractures depicted at lateral thoracic spine X-ray (A). Fractures are confirmed at CT (B–E). Dual Energy bone marrow images (C, D, E) show bone marrow edema in T9, T10, T11 and T12 vertebral bodies (blue arrows in C), indicating recent osteoporotic fractures

Case 2: A giant cell tumor of the distal femur and a recent pathological fracture (Fig. 2). The patient was a 42-year-old man with a giant cell tumor of the distal femur (osteolytic area) and a recent pathological fracture suspected at X-ray. Fracture was confirmed by conventional gray-scale CT. Bone marrow-superimposed images indicated a recent fracture.

Case 3: Lateral tibial plateau comminuted fracture suspected at conventional radiography and confirmed at DECT (Fig. 3). The patient was a 77-year-old patient with a lateral tibial plateau fracture suspected on conventional radiography. Axial and coronal CT confirmed a comminuted tibial plateau fracture. DECT with bone marrow edema-superimposed images demonstrated bone marrow edema in the lateral tibial plateau, indicating a recent fracture.

Case 4: Bilateral pulmonary embolism with multiple perfusion defects depicted on iodine maps (Fig. 4). The patient was a 61-year-old woman with bilateral pulmonary embolism at the contrast-enhanced DECT. The iodine signal was identified and color coded in red within the segmented lung. The iodine overlay image was superimposed on a gray-scale mixed image. On the 3D iodine perfusion map, the dark regions show bilateral perfusion defects secondary to embolism. The ability to obtain perfusion images using dual-source technology is one of the clear advantages of DECT over conventional computed tomography pulmonary angiography. The material decomposition theory, a method that enables the quantitative evaluation of iodine, is used to obtain a DECT perfusion scan. When it comes to diagnosing acute pulmonary emboli, DECT has many advantages over

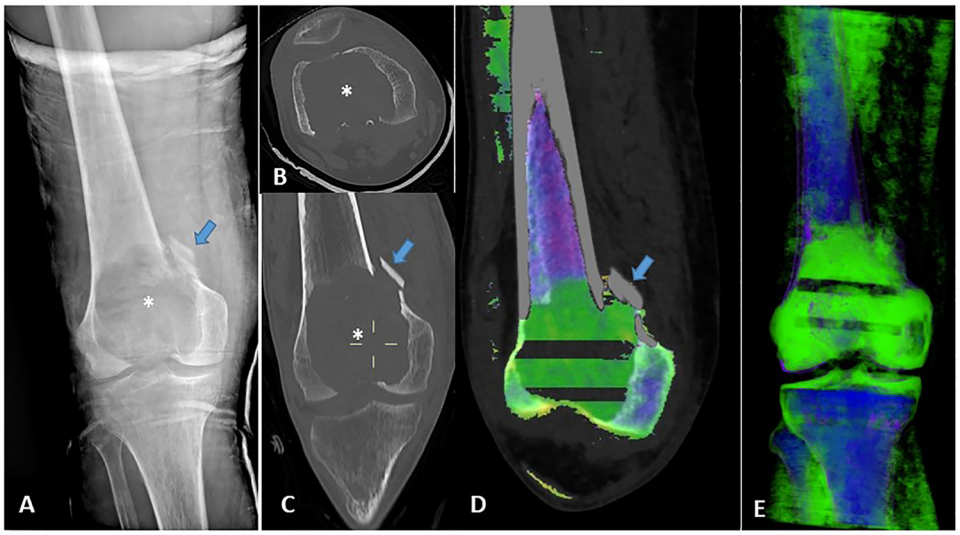

Fig. 2. 42-year-old patient with giant cell tumor of the distal femur (osteolytic area indicated by asterisks in A, B, C) and a recent pathological fracture suspected at X-Ray (A, blue arrow). Fracture is confirmed at conventional grey-scale CT (C). Bone marrow superimposed images (D, E) indicate a recent fracture

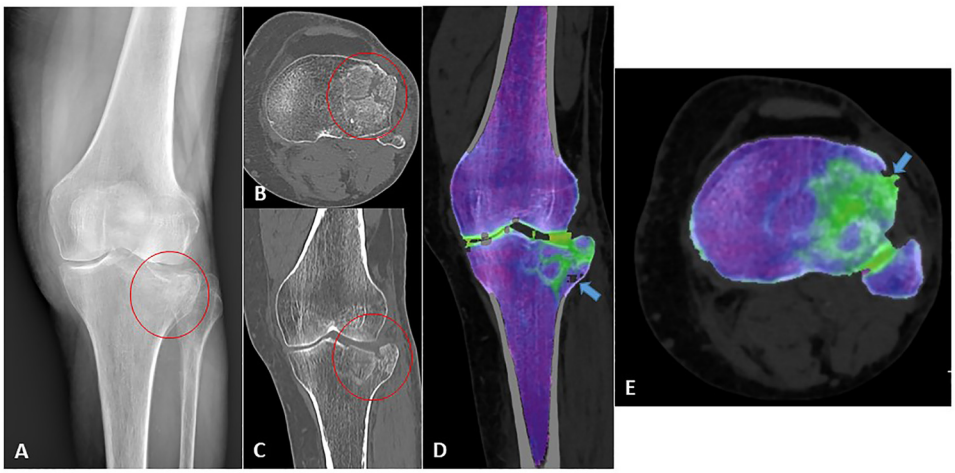

Fig. 3. 77-year-old patient with lateral tibial plateau fracture suspected at conventional radiography (red circle in A). Axial (B) and coronal (C) CT confirm comminuted tibial plateau fracture (red circles). Dual-energy CT with bone marrow edema superimposed images (D, E) demonstrates bone marrow edema in the lateral tibial plateau, indicating a recent fracture

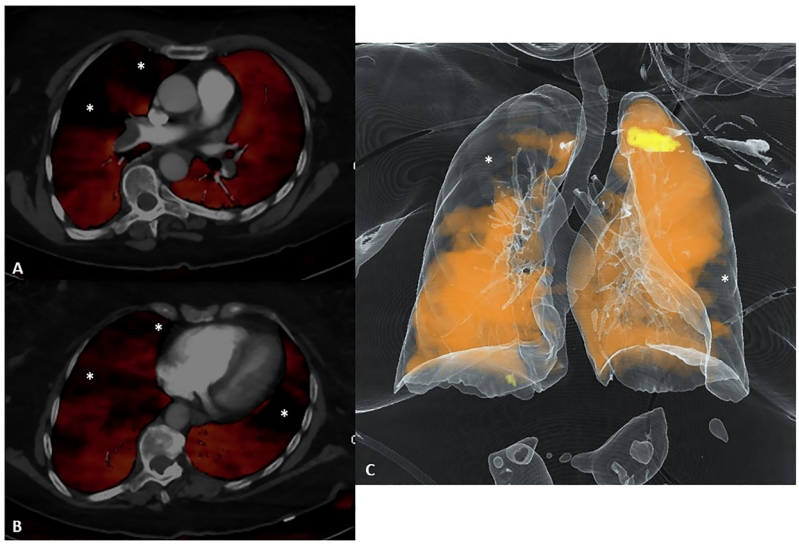

Fig. 4. Contrast-enhanced, dual-energy CT images in a 61-year-old woman with bilateral pulmonary embolism. Iodine signal is identified and color coded in red within the segmented lung. The iodine overlay image is super-imposed on a gray-scale mixed image (A–B). In C, a 3D iodine perfusion map is showed. The dark regions show bilateral perfusion defects secondary to the embolism (asterisks)

traditional CT pulmonary angiography. In fact, some of these benefits might also apply to the detection of chronic pulmonary embolism. [11].

Case 5: Metal artifact reduction and fracture rule-out in a patient with a previous total knee replacement (Fig. 5). The patient was a 70-year-old male with prior total knee replacement and a suspected periprostethic fracture after a ladder fall. Spectral mono-energetic images at 140 keV showed improvement of the metal artifacts, improving the image quality and allowing a better evaluation of the periprosthetic bone, with no fractures detected. DECT with bone marrow edema superimposed images demonstrated the absence of areas of bone marrow edema, confirming the absence of a recent fracture. DECT with specific postprocessing significantly improves the evaluation of metallic implants.

Case 6: Recent acetabular comminuted fracture (Fig. 6). The patient was a 80-year-old man with an acetabular comminuted fracture on conventional CT. DECT with bone marrow edema superimposed images demonstrated bone marrow edema in the right acetabular region, indicating a recent fracture. The ability to distinguish fresh from old fractures by demonstrating the presence of bone marrow edema, remains one of DECT's greatest advantages.

Case 7: Left sacral wing fracture with equivocal X-ray findings, confirmed at DECT (Fig. 7). The patient was a 25-year-old man with pain in the sacral region following a motorcycle accident. Sagittal reformatted CT demonstrated

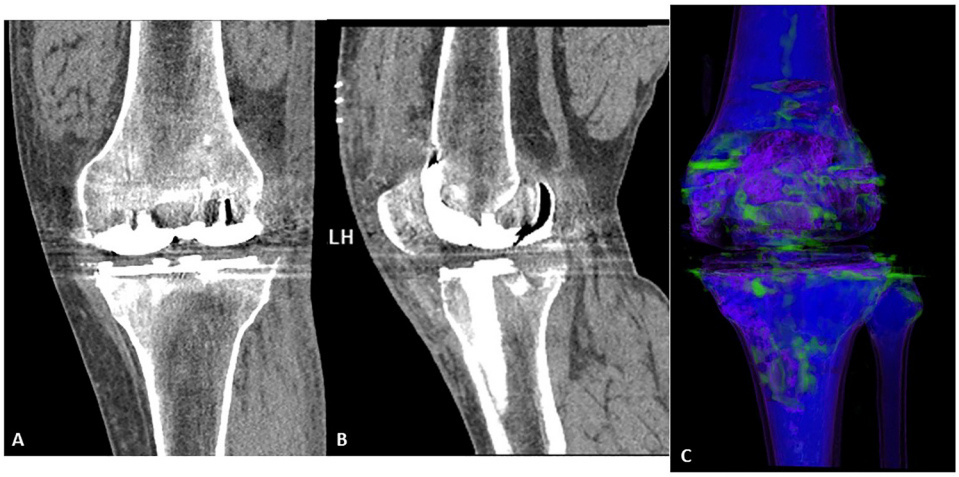

Fig. 5. 70-year-old male with prior total knee replacement and suspected periprosthetic fracture after ladder fall. Spectral mono-energetic images at 140 keV (A and B) show improvement of artifacts and allow a better evaluation of periprosthetic bone, with no fractures detected. Dual-energy CT with bone marrow edema superimposed images (C) demonstrate absence of areas of bone marrow edema, confirming the absence of a recent fracture

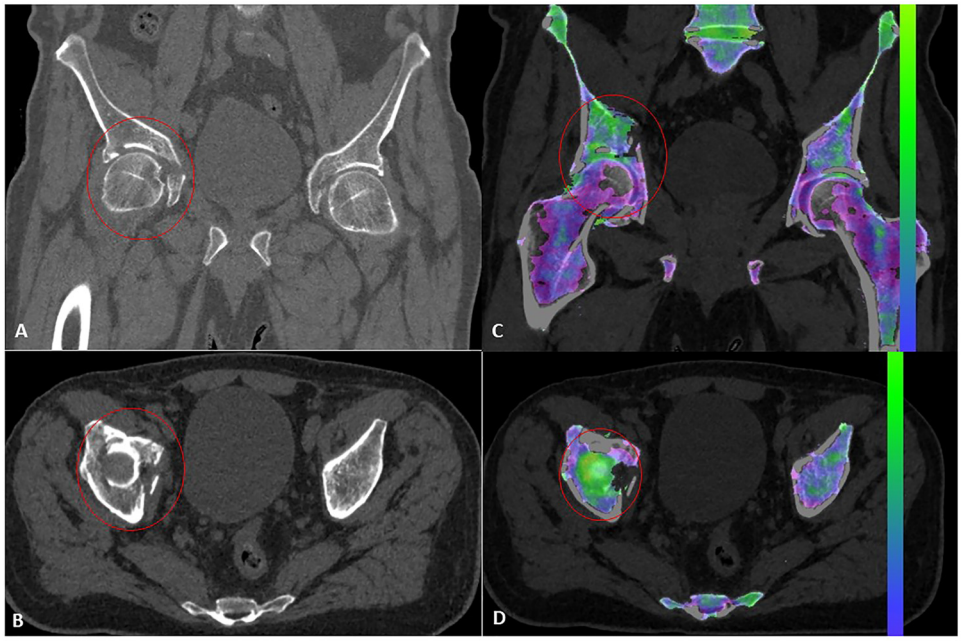

Fig. 6. 80-year-old patient with acetabular comminuted fracture at conventional CT (red circles in A and B). Dual-energy CT with bone marrow edema superimposed images (C, D) demonstrate bone marrow edema in the right acetabular region (red circles), indicating a recent fracture

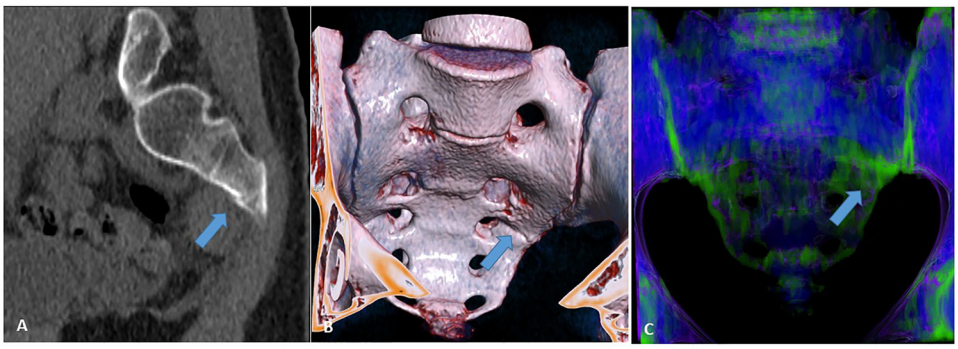

Fig. 7. 25-year-old patient with pain in the sacral region following a motorcycle accident. Sagittal reformatted CT (A) demonstrates a focal cortical discontinuity in the left sacral wing (blue arrow), which is confirmed at 3D-volume rendering reconstruction (B). Dual-energy CT with bone marrow edema superimposed images (C) demonstrate bone marrow edema in the left sacral wing (blue arrow), indicating a recent fracture

a focal cortical discontinuity in the left sacral wing, which was confirmed at 3D volume rendering reconstruction. DECT with bone marrow edema-superimposed images demonstrated bone marrow edema in the left sacral wing, indicating a recent fracture.

Case 8: Urinary stone characterization in a patient with left renal colic (Figs 8 and 9) A 52-year-old patient with left renal colic showed up at the emergency department. Axial and coronal unenhanced CT demonstrated a 2-cm stone in the left renal pelvis. DECT stone characterization showed a calcium-containing stone with a volume of 1.86cc. The patient was treated with lithotripsy and a left nephrostomy. DECT is increasingly being used to differentiate between calcium and uric acid urinary tract calculi. Predicting urinary tract calculus composition by DECT plays an

Fig. 8. 52 year-old Patient with left renal colic. Axial (A) and coronal (B) unenhanced CT demonstrate a 2 cm stone in the left renal pelvis (red circles)

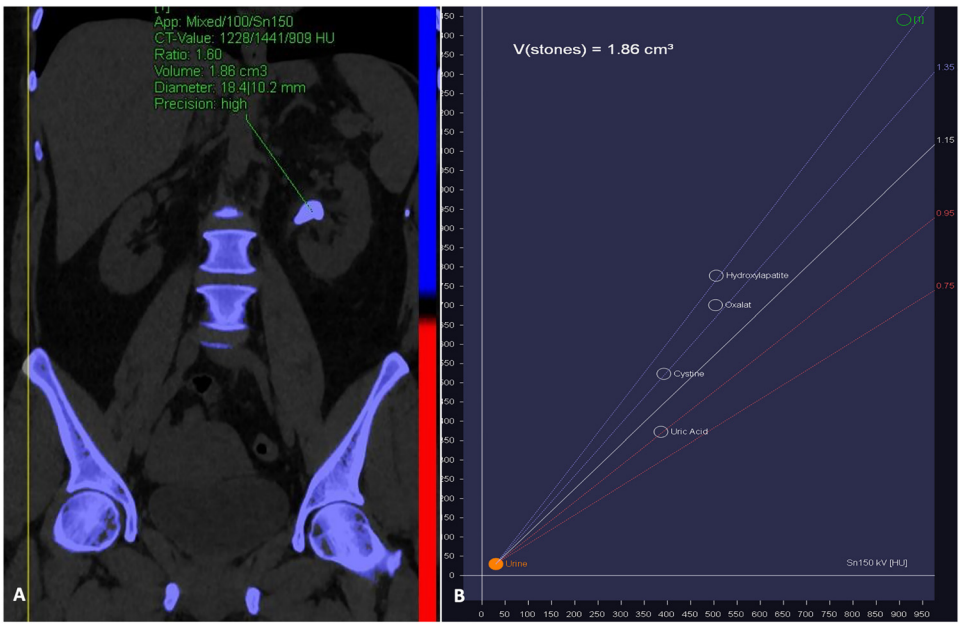

Fig. 9. Same patient as Fig. 8. Dual energy CT stone characterization (A,B) shows a calcium-containing stone with a volume of 1.86cc. The patient was treated with lithotripsy and left nephrostomy

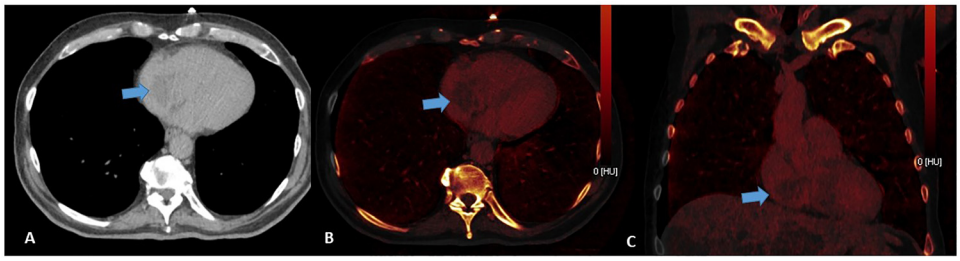

Fig. 10. 60-year-old patient with indeterminate right atrial mass. Delayed contrast-enhanced CT (A) showing lobulated hypodensity in right atrium. Dual-Energy axial and coronal iodine perfusion maps (B and C) confirm a right atrial mass with no signs of iodine uptake, suggestive for thrombus (blue arrows)

important role in identifying patients who may be managed with dissolution therapy.

Case 9: A 60-year-old patient with indeterminate right atrial mass (Fig. 10). Delayed contrast-enhanced CT (A) showed lobulated hypodensity in the right atrium. Dual-energy axial and coronal iodine perfusion maps (B and C) confirmed a right atrial mass with no signs of iodine uptake, suggesting a thrombus (blue arrows).

Conclusion

DECT is a promising imaging technique with increasing availability and multiple emerging and established clinical applications that may allow radiologists to make quicker and more precise diagnoses in the emergency setting. DECT is a constantly developing technique that provides promising results in newly emerging fields of application.

Authors' contributions: Dr. Vincenzo Cirimele: conception of the work, acquisition and analysis of the data for the work, drafting the work.

Dr. Giulia D'Amone: conception of the work, acquisition and analysis of the data for the work, drafting the work.

Prof. Carlo Mallio: reviewing the work critically for important intellectual content.

Prof. Bruno Beomonte Zobel: reviewing the work critically for important intellectual content.

Dr. Eliodoro Faiella: reviewing the work critically for important intellectual content.

All authors reviewed the final version of the manuscript and agreed to submit it to IMAGING for publication.

Funding sources: No financial support was received for this study.

Conflict of interests: The authors have no conflict of interest to disclose.

Ethical statement: All procedures performed in studies involving human participants were in accordance with the ethical standards of the institutional and/or national research committee and with the 1964 Helsinki declaration and its later amendments or comparable ethical standards.

ACKNOWLEDGEMENTS

The authors have no further information to disclose.

REFERENCES

[1] Demirler Simsir B, Danse E, Coche E: Benefit of dual-layer spectral CT in emergency imaging of different organ systems. Clin Radiol 2020 Dec; 75(12): 886–902.

[2] Adam SZ, Rabinowich A, Kessner R, Blachar A: Spectral CT of the abdomen: where are we now? Insights Imaging 2021 Sep 27; 12(1): 138.

[3] Krauss B: Dual-energy computed tomography: technology and challenges. Radiol Clin North Am 2018 Jul; 56(4): 497–506.

[4] Jamali S, Michoux N, Coche E, Dragean CA: Virtual unenhanced phase with spectral dual-energy CT: is it an alternative to conventional true unenhanced phase for abdominal tissues? Diagn Interv Imaging 2019 Sep; 100(9): 503–11.

[5] Parakh A, Macri F, Sahani D: Dual-energy computed tomography: dose reduction, series reduction, and contrast load reduction in dual-energy computed tomography. Radiol Clin North Am 2018 Jul; 56(4): 601–24.

[6] Große Hokamp N, Gilkeson R, Jordan MK, Laukamp KR, Neuhaus VF, Haneder S, et al.: Virtual monoenergetic images from spectral detector CT as a surrogate for conventional CT images: unaltered attenuation characteristics with reduced image noise. Eur J Radiol 2019 Aug; 117: 49–55.

[7] Große Hokamp N, Abdullayev N, Persigehl T, Schlaak M, Wybranski C, Holz JA, et al.: Precision and reliability of liver iodine quantification from spectral detector CT: Evidence from phantom and patient data. Eur Radiol 2019 Apr; 29(4): 2098–106.

[8] Megibow AJ, Kambadakone A, Ananthakrishnan L: Dual-energy computed tomography: image acquisition, processing, and workflow. Radiol Clin North Am 2018 Jul; 56(4): 507–20.

[9] Van Ommen F, de Jong HWAM, Dankbaar JW, Bennink E, Leiner T, Schilham AMR: Dose of CT protocols acquired in clinical routine using a dual-layer detector CT scanner: a preliminary report. Eur J Radiol 2019 Mar; 112: 65–71.

[10] Siegel MJ, Mhlanga JC, Salter A, Ramirez-Giraldo JC: Comparison of radiation dose and image quality between contrast-enhanced single- and dual-energy abdominopelvic computed tomography in children as a function of patient size. Pediatr Radiol 2021 Oct; 51(11): 2000–8.

[11] Farag A, Fielding J, Catanzano T: Role of dual-energy computed tomography in diagnosis of acute pulmonary emboli, a review. Semin Ultrasound CT MR 2022 Aug; 43(4): 333–43.